British Journal of Pharmacology (2007) 150, 541–551

0007–1188/07 $30.00
www.brjpharmacol.org

REVIEW

Taking The Time To Study Competitive Antagonism

DJA Wyllie and PE Chen

Centre for Neuroscience Research, University of Edinburgh, Edinburgh, UK

Selective receptor antagonists are one of the most powerful resources in a pharmacologist's toolkit and are essential for the identification and classification of receptor subtypes and dissecting their roles in normal and abnormal body function. However, when the actions of antagonists are measured inappropriately and misleading results are reported, confusion and wrong interpretations ensue. This article gives a general overview of Schild analysis and the method of determining antagonist equilibrium constants. We demonstrate why this technique is preferable in the study of competitive receptor antagonism than the calculation of antagonist concentration that inhibit agonist-evoked responses by 50%. In addition we show how the use of Schild analysis can provide information on the outcome of single amino acid mutations in structure-function studies of receptors. Finally, we illustrate the need for caution when studying the effects of potent antagonists on synaptic transmission where the timescale of events under investigation is such that ligands and receptors never reach steady-state occupancy.
British Journal of Pharmacology (2007) **150,** 541–551. doi:10.1038/sj.bjp.0706997; published online 22 January 2007

Keywords: agonist; antagonist; Schild analysis; equilibrium constant; inhibition; binding; gating; D-AP5; NVP-AAM077

Abbreviations: D-AP5, D-2-amino-5-phosphonopentanoic acid; NMDA, *N*-methyl-D-aspartate; NVP-AAM077, (*R*)-[(*S*)-1-(4-bromo-phenyl)-ethylamino]-(2,3-dioxo-1,2,3,4-tetrahydroquinoxalin-5-yl)-methyl]-phosphonic acid

Introduction

Quantifying the actions of ligands with their receptors is fundamental not only to our understanding of receptor pharmacology, in the classification and identification of the roles played by various receptor subtypes, but is also central to the development of selective drugs used in the treatment of disease (e.g see Rang, 2006). For those interested in a brief historical overview of quantitative approaches to the analysis of receptor pharmacology see Colquhoun (2006a). In terms of agonist action, it is common and relatively straightforward to quantify the response evoked in terms of the concentration of ligand required to give 50% of a maximum response (the EC_{50}). Nonetheless, the use of EC_{50} values to determine the nature of binding and unbinding events can be extremely complicated (e.g. see Colquhoun, 1998, 2006b). In contrast, interpretation of antagonist action and in particular reversible competitive antagonism is rather more straightforward. Specifically, a method (Schild analysis) first described almost 60 years ago allows us to determine the equilibrium constant for binding of a competitive antagonist acting at a particular receptor (Schild, 1949; Arunlakshana and Schild, 1959). Indeed, quantitative analysis of competitive antagonist action by the Schild method has been employed in the pharmacological characterization of many clinically important drugs, including histamine H_2 receptor antagonists (Black *et al*., 1972; reviewed in Black, 1993), β-adrenoceptor blockers (Black *et al*., 1965; reviewed in Black, 1993) and neuromuscular blockers (reviewed in Bowman, 2006). An alternative parameter used to quantify antagonist action is the so-called IC_{50} value of an antagonist (the concentration of antagonist required to reduce a response to a fixed concentration of agonist by 50%). Although methods of determining IC_{50} values are perhaps easier to implement than a Schild analysis, this article will discuss some of the limitations of using this measurement when studying antagonist action. Certain situations, do however, preclude Schild analysis and in such cases one needs to resort to determining IC_{50} values. For example, the stability or potency of an antagonist may prevent Schild analysis. In addition, responses evoked under non-steady-state conditions such as those resulting from the synaptic release of neurotransmitter do not lend themselves to antagonist action being studied by the Schild method.

The examples used in this review are taken from studies of ligand-gated ion channels (LGICs) rather than the far more numerous G-protein-coupled receptors (GPCRs). For LGICs it has been possible to construct simple kinetic schemes that describe several aspects of agonist and antagonist action at these receptors. For GPCRs, agonist action is far more complex, in the sense that the binding of a ligand to its receptor is only the initial step of an intricate biochemical

Correspondence: Dr DJA Wyllie, Centre for Neuroscience Research, University of Edinburgh, 1 George Square, Edinburgh EH8 9JZ, UK.
E-mail: dwyllie1@staffmail.ed.ac.uk
Received 22 September 2006; revised 26 October 2006; accepted 9 November 2006; published online 22 January 2007

cascade, which eventually leads to a biological response. Nevertheless, the same principles that are discussed in this review apply to the study of GPCRs.

The demise of Pharmacology Departments, the reduction in discipline-based teaching and the ever-declining funding for hands-on practical-based teaching in undergraduate study programmes means that the opportunities for instructing future generations of research pharmacologists are being eroded. We hope this review serves a useful purpose in highlighting some of the problems involved in conducting quantitative analysis of ligand–receptor interactions and the study of competitive receptor antagonism.

IC_{50} and K_B measurements – 'simulated' data example

Consider the kinetic scheme shown in Figure 1a. The scheme is based on the simple del Castillo and Katz (1957) reaction scheme, used first to describe the action of acetylcholine at nicotinic acetylcholine receptors (the prototypical ligand-gated ion channel) present at the neuromuscular junction. In the scheme an agonist (A) binds to its receptor (R) to form an agonist–receptor complex (AR). There is a subsequent isomerization step to denote the active (open) state of the receptor (AR*). Incorporated into this scheme is the mutually exclusive binding of an antagonist (B) to the receptor to give an inactive and blocked receptor (BR). The equilibrium constants, defined as the dissociation rate divided by the association rate, for the agonist and antagonist binding reactions are denoted by K_A and K_B, respectively, whereas the equilibrium constant for the isomerization reaction, E, is defined as the forward (opening) rate constant divided by the backward (closing) rate constant. At any given agonist and antagonist concentration (denoted as (A) and (B), respectively), the response will be proportional to the proportion, p_{AR*}, of receptors in the active state (AR*). This

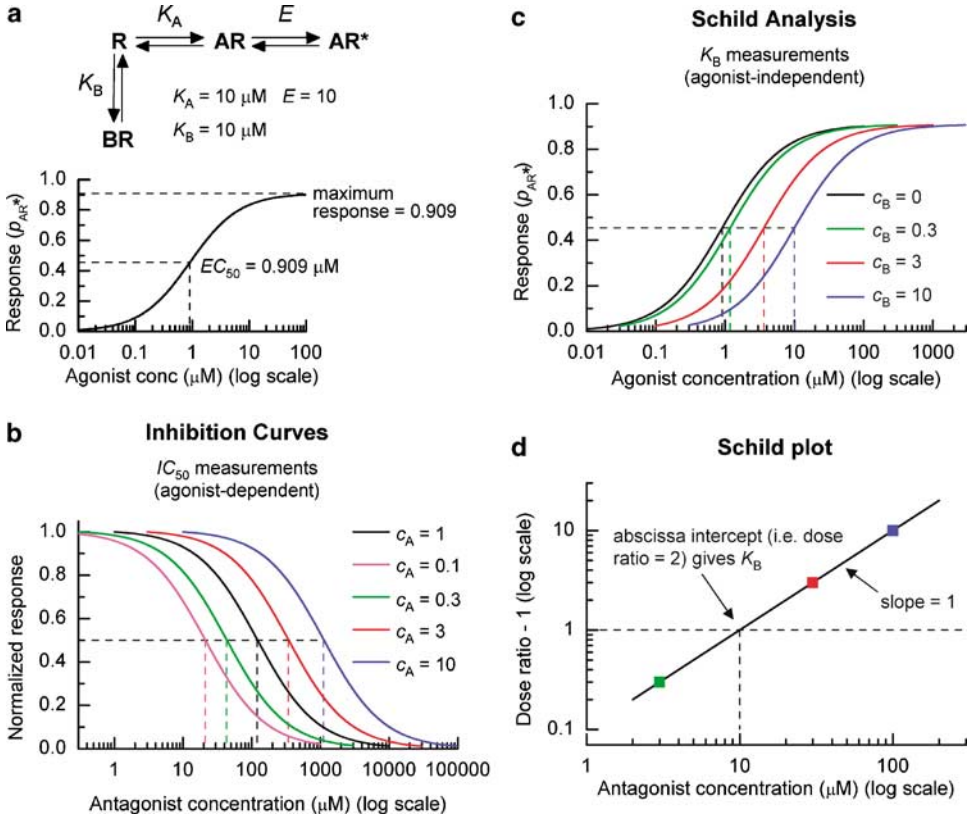

Figure 1 Methods for calculating IC_{50} and K_B Values. (**a**) Reaction scheme, based on the del Castillo–Katz mechanism, which incorporates the mutually exclusive binding of two different ligands denoted as A (agonist) and B (antagonist). In this scheme, the receptor can exist in one of three inactive states – unbound (R), bound by agonist (AR) and bound by antagonist (BR) and one active state (AR*). The equilibrium constant for agonist binding is given by K_A, whereas that for antagonist binding is given by K_B. The equilibrium constant for the isomerization reaction is denoted by E. For the simulations shown in the remaining panels the following equilibrium constants are used: $K_A = K_B = 10\ \mu M$ and $E = 10$. The plot below the reaction scheme shows the concentration–response curve (in terms of the occupancy of the AR* state, p_{AR*}) that would be obtained in the absence of antagonist. It predicts a maximum response (p_{max}) of 0.909 and an EC_{50} for the agonist of 0.909 μM. (**b**) A series of inhibition curves predicted from the reaction scheme shown in (**a**), with the normalized agonist concentration, c_A, set to be equal to 0.1, 0.3, 1, 3 and 10. For each curve, responses have been normalized to the predicted maximal response (in the absence of antagonist) for each agonist concentration used. The dashed lines indicate the predicted IC_{50} values that would be obtained for each agonist concentration. (**c**) A series of concentration–response curves that are predicted from the scheme shown in (**a**), in the absence (black curve) and presence (coloured curves) of antagonist. Note that increasing the antagonist concentrations results in a parallel shift to the right of the concentration–response curve; however, the maximum response that can be achieved is equivalent whether or not antagonist is present. The dashed lines indicate the predicted EC_{50} values that would be obtained under each condition. (**d**) Schild plot resulting from the analysis of the data represented in (**c**). The data points (colour-coded corresponding to the dose ratios obtained from the curves in (**c**)) fall on a straight line whose slope is equal to one. The intercept of this line with the abscissa (indicated by the dashed horizontal line) gives the K_B value for the antagonist.

proportion depends, as for all equilibrium expressions, only on the ratio of concentration to equilibrium constant. It is, therefore, convenient and concise to write results in terms of normalized concentrations defined as

$$c_A = \frac{[A]}{K_A} \quad \text{and} \quad c_B = \frac{[B]}{K_B} \tag{1}$$

for agonist and antagonist, respectively.

The result is,

$$p_{AR^*} = \frac{E\, c_A}{1 + c_B + c_A(1+E)} \tag{2}$$

This result (the derivation of which is shown in the Appendix) can equally be written in a slightly different form which shows that the response depends only on the ratio $c_A/(1+c_B)$, thus,

$$p_{AR^*} = \frac{E\dfrac{c_A}{(1+c_B)}}{1 + \dfrac{c_A}{(1+c_B)}(1+E)} \tag{3}$$

This form has the advantage, as will be shown below, that it makes it immediately obvious that our mechanism should obey the Schild equation as an increase in antagonist concentration can be overcome by increasing the agonist concentration by a factor $(1+c_B)$.

The maximum response (p_{max}) that can be achieved when the agonist concentration is infinitely high is given by the expression

$$p_{max} = \frac{E}{1+E} \tag{4}$$

and the concentration of agonist required to obtain a half-maximal response (EC_{50}) is given by the expression

$$EC_{50} = \frac{K_A}{(1+E)}(1+c_B) \tag{5}$$

The EC_{50} in the absence of antagonist is $K_A/(1+E)$, and this rises linearly with increasing antagonist concentration, in proportion to the 'Schild factor', $(1+c_B)$.

In Figure 1, the concentration–response curve shown below the reaction scheme (where the antagonist concentration is set to zero) is generated by setting $K_A = 10\,\mu M$ and $E = 10$. Note that the maximum response that can be achieved is not 1, but rather 0.909 ($= 10/11$, from equation (4)), and the EC_{50} value that would be observed would equal $0.909\,\mu M$ (i.e., the concentration of agonist to evoke a response of $p_{AR^*} = 0.5 p_{max} = 0.4545$).

Figure 1b shows the effect of varying the antagonist concentration in the presence of a fixed concentration of agonist (for this simulation $K_A = K_B = 10\,\mu M$ and $E = 10$). This is the method used for the generation of inhibition curves and the determination of an antagonist concentration that reduces the response (in the absence of antagonist) by a set amount – usually 50% (the IC_{50} value). The curves show the responses that are obtained when the agonist concentration is fixed at 0.1, 0.3, 1, 3 or 10 times the K_A value for the agonist (i.e., $c_A = 0.1$, 0.3, 1, 3 and 10, respectively). In addition, responses have been normalized to the maximum response that would be obtained for each agonist concentration in the absence of antagonist – these range from 0.476 ($c_A = 0.1$) to 0.901 ($c_A = 10$). The dashed lines show where the IC_{50} value would be for each set of conditions. Notice that the IC_{50} values in this (albeit extreme) example range from 21 to $1110\,\mu M$ and, without having additional information at hand, do not give a good estimate of the K_B value ($10\,\mu M$). For this mechanism, the IC_{50} is given by

$$IC_{50} = K_B(1 + c_A(1+E)) \tag{6}$$

Thus, the IC_{50} must always be bigger than the required K_B, and the higher the fixed agonist concentration, the greater the error. In contrast, as we show below, the Schild method gives K_B itself.

This example serves to illustrate a very important point about how one goes about determining IC_{50} values – they are critically dependent on the agonist concentration used. Note that while the reaction scheme we have used in this example illustrates competitive antagonism, IC_{50} values can also be obtained for antagonists that act in a non-competitive manner – thus they tell us nothing about the nature of the antagonism that is under investigation. Despite this, or indeed perhaps because of this, and the fact that generating inhibition curves and the subsequent estimation of an antagonist's IC_{50} value is a relatively quick process, inhibition curves are far more commonly reported than their usefulness (in terms of mechanistic understanding) warrants.

In contrast, the Schild method (Schild, 1949; Arunlakshana and Schild, 1959) of investigating antagonist action is not only independent of the nature, and the concentration, of the agonist used to evoke responses, but also tells us whether or not antagonism is competitive in nature and allows, when competitive antagonism is observed, for the determination of the equilibrium constant for binding of the antagonist to its receptor. This equilibrium constant is a single, physically-defined constant that characterizes the receptor. The method for undertaking Schild analysis is shown in Figure 1c and d. First one generates a concentration–response curve in the absence of antagonist (this is depicted as the black curve on the graph shown in Figure 1c). Next, in the presence of a series of increasing antagonist concentrations, further sets of concentration–response curves are obtained (coloured curves in Figure 1c). Note that the ordinate in this graph plots the actual 'response' (i.e., the proportion of receptors in the AR* state of the reaction scheme illustrated in Figure 1a) and not a normalized response (as is the case for the inhibition curves in Figure 1b). When carrying out Schild analysis it is best to try and use a wide range of antagonist concentrations so as to obtain clear 'shifts' in the agonist concentration–response curves, and also to test the range of antagonist concentrations over which competitive behaviour is seen. Next, one needs to calculate what is referred to as the 'dose ratio' (r). Simply put, this is the factor by which the concentration of agonist needs to be increased by to obtain the same response in the presence of the antagonist as was obtained in its absence. The assumption that is made here is that the same fraction of receptors need to be activated in order to obtain the same response in the absence and presence of the

antagonist, but we do not need to know what this fraction is. Putting this in terms of the reaction scheme shown in Figure 1a, this is the equivalent of solving the following equation:

$$p_{AR^*} = \frac{E\dfrac{r\ c_A}{(1+c_B)}}{1+\dfrac{r\ c_A}{(1+c_B)}(1+E)} = \frac{E\ c_A}{1+c_A(1+E)} \qquad (7)$$

where the right-hand side gives the magnitude of the response in the absence of antagonist and the left-hand side indicates the factor (dose ratio, r) by which the agonist concentration needs to be increased to obtain the same response. The solution to this equation is simply $r = 1 + c_B$, i.e.,

$$r = 1 + \frac{[B]}{K_B} \qquad (8)$$

and this is known as the Schild equation. The beautiful thing about this result shown in equation (8) is that, unlike the IC_{50} (equation (6)), it does not involve the agonist at all and nor does it involve the 'efficacy' term, E.

It is common, if a series of complete concentration–response curves are available, to use the EC_{50} concentration. The dashed lines indicate the respective EC_{50} values for each of the curves and here with our 'perfect' data set are equal to 0.909, 1.182, 3.636 and 10 μM. Thus, the corresponding dose ratios are 1.3, 4 and 11, respectively. At this stage in the process, and if the antagonism is competitive in nature, one should observe: (1) parallel shifts to the right in the concentration–response curves and (2) no decrease in the maximum response that can be achieved. This latter point is sometimes difficult to be certain about, because receptor desensitization and tachyphalaxis of tissue responses often make it impossible to obtain the same maximum response. However, clear deviation from parallel shifts in the concentration–response curves and significant depression of the maximum response achieved in the presence of increasing antagonist concentrations should alert the experimenter that the antagonism is not competitive. For a comprehensive discussion of some of the practical considerations to be taken into consideration when carrying out Schild analysis see Kenakin (1984).

In logarithmic form, the Schild equation is written as

$$\log(r-1) = \log[B] - \log K_B \qquad (9)$$

and therefore (when antagonism is competitive) a log–log plot of $r-1$ against the antagonist concentration gives a straight line with a slope equal to unity (Figure 1d). Such plots are referred to as Schild plots. The slope of the Schild plot is predicted to be unity and *only* when the slope is unity does the intercept on the abscissa give an estimate of the K_B value of the antagonist. Therefore, best practice is to fit the data points with a line of unconstrained slope and determine if this is significantly different from unity (e.g see Colquhoun, 1971). If the data are consistent with the prediction of the Schild equation the data should be refitted with a line with its slope constrained to equal one so as to obtain the K_B of the antagonist. Strictly speaking, the intercept of a line (with the abscissa), which has a slope not equal to one, gives the antagonist concentration that produces a dose ratio equal to 2, the $-\log_{10}$ of which is referred to as the pA_2 value of the antagonist, that is the negative logarithm to the base 10 of the molar concentration of the antagonist that makes it necessary to double to concentration of agonist to elicit the same (submaximal) response obtained in the absence of antagonist (Schild, 1947). Thus, even for antagonists that do not act in a competitive manner, Schild plots can be generated and pA_2 values can be determined – only when the slopes of such plots are equal to one will the pA_2 value be equal to $-\log_{10}K_B$.

Unlike the series of inhibition curves (Figure 1b), the Schild plot shown in Figure 1d returns the K_B value of the antagonist. From inspection of the Schild equation one can see that there is no parameter that is dependent on the agonist – thus Schild analysis is agonist-independent in the sense that the same K_B value will be obtained no matter the nature of the agonist used to generate the agonist concentration–response curves (of course, one must use the *same* agonist for each dataset). This is one of the great advantages of this method of analysis. Alternative (nonlinear regression) approaches to obtain K_B values have been reported and their merits discussed (e.g. see Lew and Angus, 1995); however, for the purposes of this review we are concerned specifically with the determination and usefulness of K_B rather than IC_{50} values.

Caveat emptor – Cheng-Prusoff is not a valid method to determine K_B values

Many investigators report K_B values that are derived, not from Schild analysis, but rather from the so-called Cheng-Prusoff method (Cheng and Prusoff, 1973). This method, as originally reported, was applied to studies of enzymatic reactions and gave the relationship between the concentration of an enzyme inhibitor that reduced the initial rate of reaction to 50% of that seen in the absence of the inhibitor and the K_i of the inhibitor. It is essentially a correction for having failed to fit the correct competitive equations to the data in the first place. Notwithstanding its derivation, this method has been adopted, by some pharmacologists, to convert IC_{50} values of antagonists to K_B values. Although the application of this method may, under certain conditions, *appear* to give estimates of K_B values that are similar to those determined by Schild analysis this approach is flawed (e.g. see Craig, 1993; Lazareno and Birdsall, 1993; Leff and Dougall, 1993). Briefly, as pointed out above, determination of IC_{50} values from inhibition curves tells us nothing about the nature of the antagonism – it is possible to determine a concentration of a non-competitive or irreversible antagonist that reduces an agonist-evoked response by 50%, but completely meaningless to try to translate this to a K_B value. Next, while reports have documented similarities between the Schild method and Cheng-Prusoff conversions, these occur only under quite a limited number of conditions. For example, considerable errors arise when agonist concentration response curves are not well-described by a simple rectangular hyperbola (i.e., when the Hill slope of the agonist concentration–response curve is equal to one), when the agonist concentration used to evoke responses is less

than or equal to the EC_{50} concentration and in the case of GPCRs significant errors arise when there is a low number of 'spare receptors' (e.g. see Lazareno and Birdsall, 1993). The bottom line is simply this: if one wants to demonstrate competitive antagonism and determine K_B values, use Schild analysis.

IC_{50} and K_B measurements – 'real' data example

The simulation described above looks very good in principle, but biology tends to get in the way at times so let us examine some 'real' data that support some of the points that have been made so far. Figure 2 shows data obtained from the study by Frizelle *et al*. (2006) of receptor antagonism at recombinant *N*-methyl-D-aspartate receptors (NMDARs). Figure 2a,b shows sets of steady-state inhibition curves illustrating the antagonism produced by (*R*)-[(*S*)-1-(4-bromo-phenyl)-ethylamino]-(2,3-dioxo-1,2,3,4-tetrahydroquinoxalin-5-yl)-methyl]-phosphonic acid (NVP-AAM077) acting at either rat recombinant NR1/NR2A (Figure 2a) or NR1/NR2B (Figure 2b) NMDARs expressed in *Xenopus laevis* oocytes. For each receptor combination, the concentrations (fixed) of agonist used to evoke responses were equal to the EC_{50} value or 10 times the EC_{50} value of glutamate acting at each receptor subtype. If one does not take care to use 'matched' concentrations of agonist when studying different receptor combinations then, and as pointed out above, the resulting

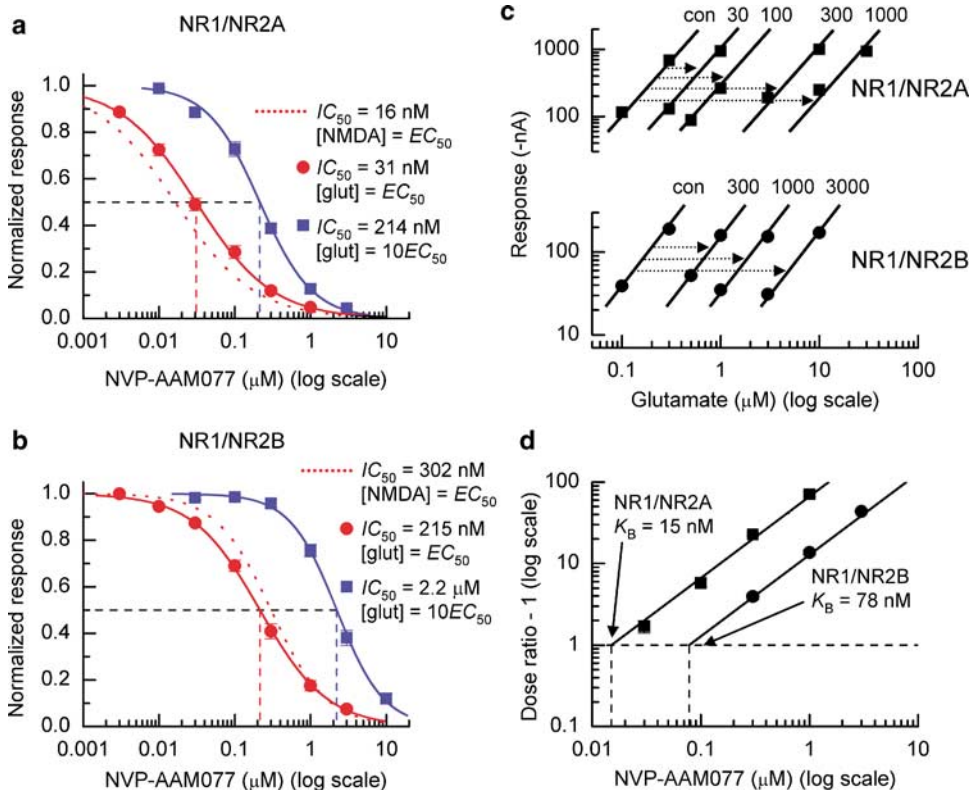

Figure 2 Comparison of IC_{50} and K_B values of a competitive antagonist at two NMDA receptor subtypes. (**a**) Mean inhibition curves to determine the IC_{50} of NVP-AAM077 acting at NR1/NR2A NMDARs and obtained when either 3 μM (= EC_{50}) glutamate (red curve) or 30 μM (= 10EC_{50}) glutamate (blue curve) was used to activate NR1/NR2A NMDA receptors. Values of the IC_{50} for NVP-AAM077 are 31 nM (for 3 μM glutamate) and 215 nM (for 30 μM glutamate). The curve shown as a dotted red line indicates the inhibition curve obtained when NMDA, rather than glutamate, was used as the agonist. Notice that NVP-AAM077 is more potent at inhibiting NR1/NR2A NMDARs activated by an EC_{50} concentration of NMDA than it is at inhibiting responses evoked by glutamate at its EC_{50} concentration. (**b**) Mean inhibition curves to determine the IC_{50} of NVP-AAM077 acting at NR1/NR2B NMDARs and obtained when either 1.5 μM (= EC_{50}) glutamate (red curve) or 15 μM (= 10EC_{50}) glutamate (blue curve) was used to activate NR1/NR2A NMDARs. Values of the IC_{50} for NVP-AAM077 are 215 nM (for 1.5 μM glutamate) and 2.2 μM (for 15 μM glutamate). The curve shown as a dotted red line indicates the inhibition curve obtained when NMDA, rather than glutamate, was used as the agonist. Notice that NVP-AAM077 is less potent at inhibiting NR1/NR2B NMDARs activated by an EC_{50} concentration of NMDA than it is at inhibiting responses evoked by glutamate at its EC_{50} concentration. (**c**) Upper panel, example of partial, low-concentration, glutamate concentration–response curves used to estimate dose ratios and obtained from an oocyte expressing NR1/NR2A NMDARs. The slope of the fitted line to the control responses (no NVP-AAM077) was constrained and used to fit the responses obtained in the presence of 30, 100, 300 nM and 1 μM NVP-AAM077. Lower panel, example of partial, low-concentration, glutamate concentration–response curves used to estimate dose ratios and obtained from an oocyte expressing NR1/NR2B NMDARs. Again, the slope of the fitted line to the control responses was constrained and used to fit the responses obtained in the presence of 300 nM, 1 μM and 3 μM NVP-AAM077. (**d**) Schild plot for antagonism of NR1/NR2A and NR1/NR2B NMDARs by NVP-AAM077 using dose ratios estimated from a series of experiments such as those illustrated in (**c**). The solid lines show fits of the data points to the Schild equation (i.e., the slopes are equal to unity). The intercept on the abscissa (where the $\log_{10}$ value of the dose ratio equals zero) gives a K_B value for NVP-AAM077 of 15 nM for NR1/NR2A NMDARs and 78 nM for NR1/NR2B NMDARs. Data adapted and reproduced, with permission, from Frizelle *et al.* (2006) ©2006 American Society for Pharmacology and Experimental Therapeutics.

IC_{50} values cannot be compared directly. Indeed, just as predicted from Figure 1b the IC_{50} values for NVP-AAM077 are dependent on the agonist concentration used to activate the particular NMDAR subtypes,. Moreover, if one was careless enough to use 30 μM glutamate ($=10EC_{50}$ value) for a study of NR1/NR2A NMDARs and only 1.5 μM glutamate ($=EC_{50}$ value) for an investigation of NR1/NR2B NMDARs, then it would be concluded that there is no difference in the potency of NVP-AAM077 at these two NMDAR subtypes. Nevertheless, the important point to note here is that when one compares, from different studies, published IC_{50} values it is essential to check, at the very least, that these have been determined at equi-potent agonist concentrations. Another aspect of the agonist-dependency of IC_{50} values is illustrated in Figure 2a and b – this concerns the nature of the agonist used to activate the receptor population. The dotted curves in each of these panels show the fit of data points (omitted for clarity; but see Frizelle *et al.*, 2006) where NMDA, rather than glutamate, is used to activate either NR1/NR2A or NR1/NR2B NMDARs. Notice that despite using equi-potent concentrations of NMDA at the two receptor subtypes, the IC_{50} values for NVP-AAM077 obtained are significantly different from those values obtained when a corresponding (i.e., equi-potent) concentration of glutamate is used. Of course, such a result is not unexpected, as IC_{50} values will be dependent upon not only the association and dissociation rate constants for the antagonist, but also those of the agonist. Indeed not only will these vary for different agonists and different receptor subtypes, but parameters such as those describing 'gating' and desensitization reactions will depend on the nature of the agonist.

Schild analysis, however, does not suffer from such problems and a method for determining the K_B for NVP-AAM077 at these two NMDAR subtypes is shown in Figure 2c and d. In Figure 2c a series of two-point concentration–response curves obtained either in the absence or presence of NVP-AAM077 are illustrated. Note that these are displayed on a log–log scale rather than the more conventional semi-logarithm display of concentration–response curves. This results in the sigmoidal shape of the concentration–response curve being transformed such that it becomes linear at low concentrations ($\ll EC_{50}$). Thus, one is able to generate with only a few data points a data set containing a series of concentration–response curves at a variety of agonist concentrations (e.g. see Colquhoun *et al.*, 1979; Evans *et al.*, 1982; Lewis *et al.*, 1997; Anson *et al.*, 1998; Frizelle *et al.*, 2006). Such a method is extremely valuable when, for example, amounts of the antagonist under investigation are limited, or where the nature of the recording does not allow for 'full' concentration–response curves to be generated, for example, electrophysiological recordings where it is not always possible to maintain recordings for sufficient time to collect a full data set. Indeed, using this sort of approach allows K_B values to be determined with a similar number of data points as is required to generate an inhibition curve. Thus, the criticism that carrying out Schild analysis is more time-consuming or requires many sample points is removed (e.g. see Lew and Angus, 1995) – one needs, however, to be careful when selecting the agonist concentrations used to evoke responses to ensure they fall on the approximately linear part of the log–log concentration–response curve.

For both receptor subtypes, increasing the concentration of NVP-AAM077 results in parallel shifts to the right of the two-point concentration–response curves. The dose ratios for each antagonist concentration are measured (as indicated by the dashed arrows) and the results are depicted as a Schild plot in Figure 2d. For both receptor subtypes, the data points fall on a straight line. Fitting a line with an unconstrained slope should first be attempted to determine whether the slopes of the lines are significantly different from one and, if not (as is the case with this example), should be re-fitted with a line whose slope is constrained to unity. The estimates of the K_B for the antagonist acting at each receptor combination can then be obtained. In this example, we see that NVP-AAM077 is approximately fivefold more potent at NR2A-containing NMDARs compared with NR2B-containing NMDARs. Furthermore, by showing that the slope of the Schild plot is equal to unity, that the antagonism is competitive, we have determined a parameter that describes the interaction of the antagonist with its binding site – neither of which we obtain from IC_{50} measurements. One might argue that using low concentrations of agonist and plotting concentration response curves on a log–log scale that one of the features of reversible competitive antagonism is not observed – namely the fact that the antagonism is surmountable, that is, a maximum response can still be achieved if one applies sufficient amounts of agonist. It is, however, a relatively straightforward matter to check this by applying increasing agonist concentrations in the presence of antagonist to ensure that a maximal response is retained (e.g. see Frizelle *et al.*, 2006).

So far we have only described the methods of how one goes about determining K_B values using Schild analysis and the merits of this approach compared with calculations of IC_{50} values. Next, we shall consider how using Schild analysis to investigate antagonist action at receptors carrying mutations can provide insights into how particular mutations bring about reductions in receptor function.

Using Schild analysis to identify the effects of mutations

Introducing point mutations into receptors is a useful experimental approach used to give insight into structure–function relationships. Nevertheless, the interpretation of such mutations is not necessarily straightforward. For receptor channels this is referred to as the 'binding-gating' problem and it has been discussed in detail (e.g. see Colquhoun, 1998, 2006b). It is exemplified in the series of concentration–response curves illustrated in Figure 3a. The black-coloured curve is the same relationship illustrated in Figure 1a and is the concentration–response curve for the del Castillo–Katz reaction scheme with $K_A = 10\,\mu$M and $E = 10$. Both the blue and red curves show shifts in the potency of the agonist, but only the shift in the EC_{50} value of the red curve results from an alteration in K_A (fivefold increase compared to black curve). The blue curve results from a fivefold reduction in the value of E, the equilibrium constant

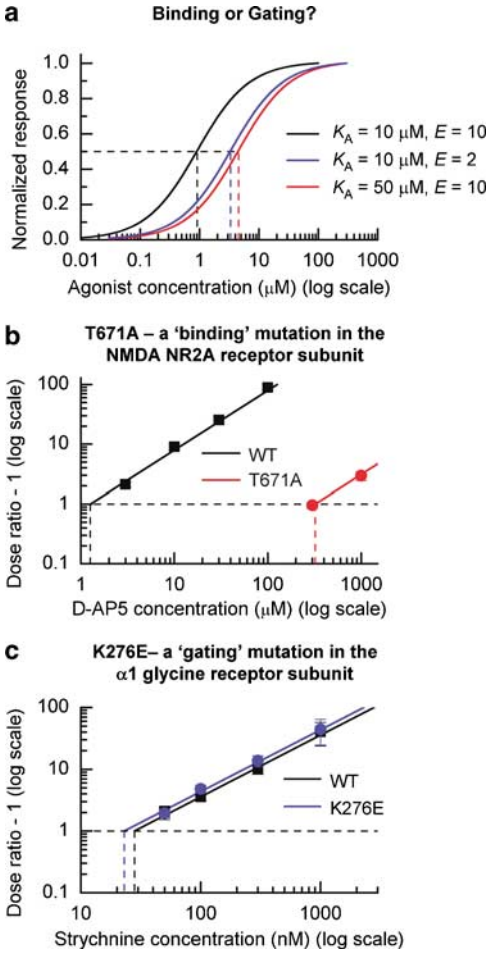

Figure 3 The 'binding-gating' problem – using competitive antagonists to investigate the effects of mutations. (**a**) Concentration–response curve (black-coloured line) predicted from the reaction scheme shown in Figure 1a. The blue- and red-coloured curves show the effect of altering either the equilibrium constant for the gating reaction (blue) or binding reaction (red). In each case, a consequence of these changes is to reduce agonist potency. (**b**) Schild plot illustrating the action of D-AP5 acting at recombinant NR1/NR2A NMDARs expressed in *X. laevis* oocytes. The point mutation NR2A(T671A) results in an increase in the K_B of the antagonist from 1.3 μM (WT) to 321 μM (mutant). (**c**) Schild plot illustrating the action of strychnine acting at recombinant α1 glycine receptors expressed in *X. laevis* oocytes. The point mutation α1(K276E) does not significantly alter the K_B of the antagonist when compared to its action at α1(WT) receptors ($K_B = 28$ nM (WT); $K_B = 23$ nM (α1(K276E)). Data in (**b**) reproduced, with permission, from Anson *et al.* (1998) ©1998 Society for Neuroscience and data in (**c**) kindly supplied by D Colquhoun (Pharmacology, UCL) and reproduced, with permission, from Lewis *et al.* (1998), ©1998 Blackwell Publishing.

for the isomerization reaction. Thus, the EC_{50} values that would be observed are 0.909 μM (black curve), 3.333 μM (blue curve) and 4.545 μM (red curve). When presented with such data, a too common, albeit naive, assumption is to attribute shifts in the potency of both curves to alterations in binding parameters. Notice that the concentration–response curves in Figure 3a have been normalized to their respective maxima. Thus, while the (predicted) maximum responses for the black and red curves are the same (0.909), that of the blue curve is less (0.666). One might argue that the fact that a reduction in E leads to a reduction in the maximum response of the system and this should alert the experimenter to the possibility that there has been an alteration in gating rather than binding parameters. However, it is never possible to ensure the same levels of receptor expression between cells (tissues) and thus clear evidence for the depression of a maximum response, when compared to wild-type (WT) or another true binding mutation, can be difficult to obtain. In any case, if the gating constant (E) is large for both of the receptors being compared, large changes in E result in only small changes in the maximum response. Inasmuch as agonist and (competitive) antagonists binding sites are formed by many of the same amino acids that make up the ligand-binding pocket, the use of Schild analysis, by allowing us to investigate antagonist action at such receptors, provides us with evidence as to whether mutations have indeed altered ligand binding. Two such examples are discussed below.

The ligand binding pocket of NMDARs is formed by two domains termed S1 and S2, which are located before the first membrane spanning region and between the second and third membrane spanning regions, respectively (reviewed in Chen and Wyllie, 2006; Mayer, 2006). The recent elucidation of the crystal structure of this region has identified the amino acids that are thought to H-bond with glutamate when it occupies the binding site (Furukawa *et al.*, 2005). Before this study, investigators introduced mutations into regions of the various NR2 NMDAR subunits and which were thought to participate in ligand binding (e.g. see Laube *et al.*, 1997, 2004; Anson *et al.*, 1998; Chen *et al.*, 2005; Hansen *et al.*, 2005; Kinarsky *et al.*, 2005) and determined whether agonist potencies were shifted as a consequence of the mutation. However, as pointed out above, shifts in agonist potency alone are not generally sufficient to interpret the role of a particular amino acid residue.

The S2 domain of all NR2 NMDAR subunits contains a pair of conserved serine–threonine residues, which H-bond with the γ-carboxyl group of glutamate. In the NR2A NMDAR subunit, mutation of either residue results in a large shift in the potency of glutamate, with an 800-fold reduction in potency being achieved when threonine (T) at position 671 is mutated to an alanine (A) residue (e.g. see Anson *et al.*, 1998; Chen *et al.*, 2005; Wyllie *et al.*, 2006). Schild analysis of the NR2A(T671A) mutation provides evidence that this reduction in potency is a consequence of an alteration in the binding site for glutamate, rather than in the coupling of binding to the gating process. NMDARs are blocked by the competitive antagonist D-2-amino-5-phosphonopentanoic acid (D-AP5) – proof that the antagonism was indeed competitive, demonstrated by Schild analysis by Evans *et al.* (1982) – and this antagonist's action at NR1/NR2A(WT) or NR1/NR2A(T671A) NMDARs is illustrated in Figure 3b. At each receptor, D-AP5 acts in a competitive manner (as judged by the slope of the line describing the data points in the Schild plot), but the value of the equilibrium constant at NR2A(T671A)-containing NMDARs is around 220-fold more than that seen at NR2A(WT)-containing NMDARs (i.e., the affinity of the antagonist is 220-fold less than that seen at NR2A(WT) receptors). Such a result is consistent with the idea that this threonine residue forms part of the ligand-

binding site of NR2 NMDAR subunits as it is to be expected that many of the residues involved in the binding of (competitive) antagonists will also play a role in the binding of agonists.

Hyperekplexia (Startle disease) is a rare genetic condition that is associated with mutations of the α subunit of the glycine-receptor ion channel. The mutation, αK276E (where the lysine residue at position 276 is replaced by a glutamic acid residue in the α subunit), has been identified as one that produces this disease. Expression of α1(K276E) receptors in *X. laevis* oocytes results in a 14-fold reduction in glycine potency when compared to glycine action at α1(WT) receptors. The maximum response that can be achieved (with equivalent levels of receptor expression) is also reduced with the α1(K276E) mutation, which suggests that, in part, the effect of this mutation is to alter gating of the receptor–channel complex. Thus, if the main effect of this mutation is on channel gating then a prediction might be that this mutation would not affect the ability of a competitive antagonist to bind to this receptor. This has been examined in the case of the glycine-receptor competitive antagonist, strychnine (Lewis *et al*., 1997). Figure 3c shows Schild plots for strychnine action at either α1(WT) glycine receptors (black line) or α1(K276E) glycine receptors (blue line). For each receptor, the estimated K_B values for antagonist action are not significantly different (28 nM, WT; 23 nM (K276E)). Thus, to the extent that glycine and strychnine-binding sites overlap, Schild analysis has confirmed that reduction in glycine potency seen with this mutation is not due to an effect on the binding site, but rather is more likely to be due to an effect on the transduction mechanism that leads to channel opening.

Thus, Schild analysis not only provides us with a method of differentiating between receptor subtypes (and therefore the information about how the ligand-binding site in such subtypes may vary), but also gives us insights into the effects of mutations and allows us to make predictions of structure–function relationships within the receptor. In the final section of this review, we shall consider briefly what happens when the occupancy of receptors by ligands does not achieve a steady state.

A note of caution for those in a hurry

'More haste, less speed' goes the proverb. In terms of competitive antagonists, the analogy might be something like 'Less time, more block'. Everything that has been discussed above applies only to systems in equilibrium. Thus, when ligands and receptors are not in equilibrium (as is the case, e.g., during synaptic transmission) then extra care needs to be taken. The problem is exemplified in Figure 4.

Figure 4a shows a more complicated reaction scheme to describe the binding of an agonist (A) and an antagonist (B) with a receptor. The scheme is based on a kinetic model used to describe the activation of NMDARs by glutamate (e.g. see Erreger *et al*., 2005). Ignore, for the moment, the part of the scheme describing antagonist binding (denoted in red). In this scheme, there are two binding sites for the agonist to reflect the fact that each NMDARs contains two NR2 subunits, each of which can bind a molecule of agonist. The doubly occupied receptor (A_2R) can enter one of two 'desensitized' states (long-lived shut states), or via two different routes can enter a single open state (A_2R^*). Just like the AR* state in the del Castillo–Katz scheme, this is the only state that gives a 'response'. 'Synaptic-like' responses can be obtained from this kinetic scheme by applying agonist for a brief amount of time with the rate constants set to the values indicated in the figure legend (see also Erreger *et al*., 2005). The simulated response of a 1000 receptors to an application of agonist (10 mM) for a duration of 1 ms is illustrated in Figure 4b by the black-coloured trace. The point to note here is that during synaptic transmission, the duration for which receptors are exposed to neurotransmitter liberated from presynaptic nerve terminals is very short. This is quite different from the bath-application of agonist to tissue preparations carried out during *in vitro* experiments. To this system we now need to add the complication of a second ligand, in this case a competitive antagonist. The reactions in the scheme in Figure 4a shown in red illustrate the additional states that are introduced. As we are dealing with a competitive antagonist, the binding of an antagonist molecule will prevent the binding of an agonist molecule to the same binding site. Thus, in the presence of agonist and antagonist ligands the additional states of BR (singly occupied by antagonist), B_2R (doubly occupied by antagonist) and BRA (receptor occupied by one antagonist and one agonist molecule) need to be added. For the points we highlight below, we have set the equilibrium constant of the antagonist to be equal to 15 nM (with the association rate constant, $k_{+B} = 10\,\mu M^{-1}\,s^{-1}$ and the dissociation rate constant, $k_{-B} = 0.15\,s^{-1}$).

Figure 4b shows the response of a 1000 receptors to the same agonist application (10 mM for 1 ms), but now in the presence of increasing concentrations of antagonist (3, 30 and 300 nM; green, red and blue traces, respectively). In this simulation, the various antagonist concentrations were pre-applied so as to ensure equilibrium between antagonist and receptor populations, as would normally be the case if such an experiment was carried out for real. The extent of the block of the agonist-evoked response is far greater than might be predicted from the K_B of the antagonist and the high concentration of agonist that is present (10 mM). For example, at an antagonist concentration of 30 nM ($=2K_B$) approximately 80% block is achieved. This high degree of block is a consequence of the fact that the brief application of agonist is not long enough to allow an agonist–antagonist–receptor equilibrium to be established and serves to illustrate that competitive antagonists with low K_B values act irreversibly on a 'synaptic' timescale and hence, in a sense the effective potency increases (for further discussion of this point, see Frizelle *et al*., 2006).

Figure 4c shows that the concentration of agonist used in the simulation is more than sufficient to overcome the receptor block, provided the system is allowed to reach equilibrium. Thus, for each antagonist concentration, the same steady-state level of response is achieved at the end of a 60 s application of agonist. Obviously, the rate at which this is obtained will be slower for the responses evoked in presence of higher antagonist concentrations (compare the

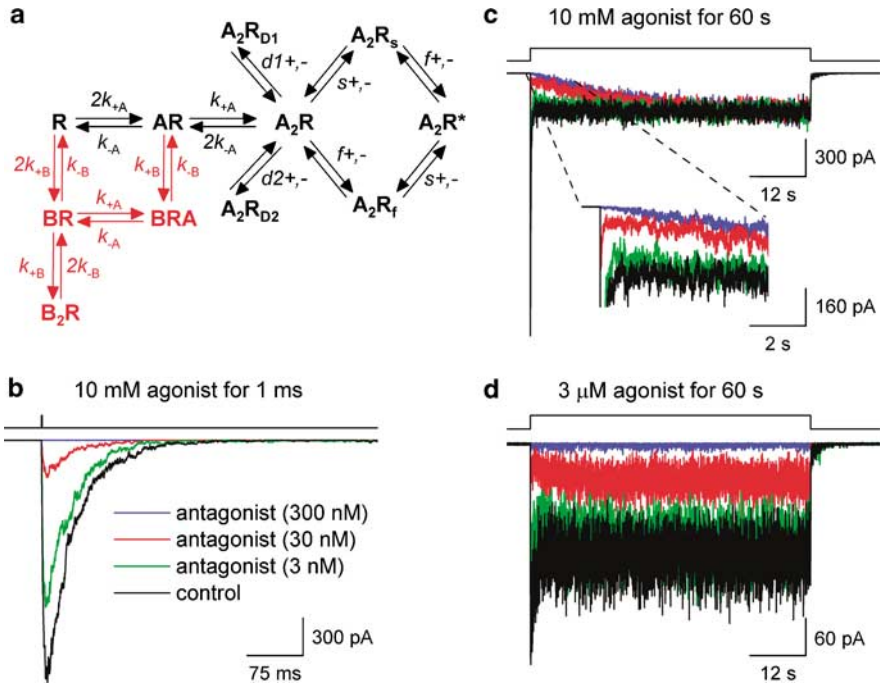

Figure 4 Reducing the duration of agonist application increases antagonist potency. (**a**) Kinetic scheme used to simulate 'synaptic' responses illustrated in (**b**). In the reaction scheme, each receptor subunit (denoted by R) can be occupied by either agonist (A) or antagonist (B). The doubly liganded A_2R state undergoes two conformation changes before channel opening (A_2R^*; for further details see Banke and Traynelis, 2003; Erreger *et al.*, 2005). Two desensitized states also exist (D1 and D2). The rate constants used in the simulation were: $k_{+A} = 2.83\,\mu M^{-1}\,s^{-1}$; $k_{-A} = 31.8\,s^{-1}$; $k_{D1+} = 85.1\,s^{-1}$; $k_{D1-} = 29.7\,s^{-1}$; $k_{D2+} = 230\,s^{-1}$; $k_{D2-} = 1.01\,s^{-1}$; $k_{s+} = 230\,s^{-1}$; $k_{s-} = 178\,s^{-1}$; $k_{f+} = 3140\,s^{-1}$; $k_{f-} = 174\,s^{-1}$; $k_{+B} = 10\,\mu M^{-1}\,s^{-1}$ and $k_{-B} = 0.15\,s^{-1}$. (**b**) Output of the kinetic scheme shown in (**a**) when 1000 channels with a conductance of 50 pS (i.e., equivalent to a single-channel amplitude of −5 pA, when the driving force is equal to −100 mV) are activated by 1 ms application of agonist (10 mM). The black trace shows the response in the absence of antagonist while the responses evoked by the agonist in the presence of 3, 30 and 300 nM antagonist are indicated by the green, red and blue curves respectively. (**c**) Equivalent simulation as shown in (**b**), but with the agonist application increased to 60 s. Notice that in each case a maximal steady-state response can be achieved although the rate at which this equilibrium is reached is dependent on the antagonist concentration. (**d**) Equivalent simulation to that shown in (**c**) with the exception that the agonist concentration has been reduced to 3 μM. In this example the steady-state level of the current is reduced in an antagonist concentration-dependent manner.

responses illustrated in the expanded view). Thus, a second important point to be made here is that equilibrium of receptor populations with agonist and antagonist can take considerable time. If this experiment was carried out for real and agonist applications made for 20 s this would not result in the system being studied at equilibrium.

Clearly, when the agonist concentration is reduced to lower concentrations, it is unable to overcome the receptor blockade produced by the antagonist. This is exemplified in Figure 4d where the agonist concentration has been set at 3 μM and the plateaus of each of the responses shows that, as is to be expected, no matter how long the agonist application a response equal to that obtained in the absence of antagonist can not be achieved.

Conclusions

As stated in the Introduction, analysis of ligand–receptor interactions is at the core of both basic and applied pharmacology. Agonist action, however, is extremely difficult to understand in terms of the rates at which an agonist binds to and unbinds from its receptor. Where this has been done it has been mainly for LGICs where there is a fuller, albeit still incomplete, understanding of transduction mechanisms leading from agonist binding to channel opening. In contrast, quantifying antagonist action can be far more straightforward. In the case of reversible competitive antagonism, Schild analysis provides us with a method for calculating the equilibrium constant for antagonist binding – indeed, it is often said that one definition of a pharmacologist is someone who can apply appropriately and understand Schild analysis.

Acknowledgements

We are grateful to the Biotechnology and Biological Sciences Research Council, The Wellcome Trust and the Honours Pharmacology Undergraduate Programme at the University of Edinburgh who have funded aspects of the work described in this review. We also thank Professor D Colquhoun and Professor JS Kelly for constructive and critical comments on the manuscript.

Conflict of interest

The authors state no conflict of interest.

References

Anson LC, Chen PE, Wyllie DJA, Colquhoun D, Schoepfer R (1998). Identification of amino acid residues of the NR2A subunit that control glutamate potency in recombinant NR1/NR2A NMDA receptors. *J Neurosci* **18**: 581–589.

Arunlakshana O, Schild HO (1959). Some quantitative uses of drug antagonists. *Br J Pharmacol Chemother* **14**: 48–57.

Banke TG, Traynelis SF (2003). Activation of NR1/NR2B NMDA receptors. *Nat Neurosci* **6**: 144–152.

Black JW (1993). Drugs from emasculated hormones: the principles of syntopic antagonism. In: Frängsmyr T, Lindsten J (eds). *Noble Lectures, Physiology or Medicine 1981–1990*. World Scientific Publishing Co.: Singapore.

Black JW, Duncan WAM, Durant CJ, Ganelin CR, Parsons EM (1972). Definition and antagonism of histamine H_2-receptors. *Nature* **236**: 385–390.

Black JW, Duncan WA, Shanks RG (1965). Comparison of some properties of pronethalol and propranolol. *Br J Pharmacol Chemother* **125**: 577–591.

Bowman WC (2006). Neuromuscular block. *Br J Pharmacol* **147**: S277–S286.

Chen PE, Geballe MT, Stansfeld PJ, Johnston AR, Yuan H, Jacob AL *et al*. (2005). Structural features of the glutamate binding site in recombinant NR1/NR2A *N*-methyl-D-aspartate receptors determined by site-directed mutagenesis and molecular modeling. *Mol Pharmacol* **67**: 1470–1484.

Chen PE, Wyllie DJA (2006). Pharmacological insights obtained from structure-function studies of ionotropic glutamate receptors. *Br J Pharmacol* **147**: 839–853.

Cheng Y, Prusoff WH (1973). Relationship between the inhibition constant (K_i) and the concentration of inhibitor which causes 50 per cent inhibition (I_{50}) of an enzymatic reaction. *Biochem Pharmacol* **22**: 3099–3108.

Colquhoun D (1971). *Lectures on Biostatistics*. Oxford: Clarendon Press; London, New York: Oxford University Press.

Colquhoun D (1998). Binding, gating, affinity and efficacy: the interpretation of structure-activity relationships for agonists and of the effects of mutating receptors. *Br J Pharmacol* **125**: 924–947.

Colquhoun D (2006a). The quantitative analysis of drug–receptor interactions: a short history. *Trends Pharmacol Sci* **27**: 149–157.

Colquhoun D (2006b). Agonist-activated ion channels. *Br J Pharmacol* **147**: S17–S26.

Colquhoun D, Dreyer F, Sheridan RE (1979). The actions of tubocurarine at the frog neuromuscular junction. *J Physiol (London)* **293**: 247–284.

Craig DA (1993). The Cheng-Prusoff relationship: something lost in the translation. *Trends Pharmacol Sci* **14**: 89–91.

del Castillo J, Katz B (1957). Interaction at end-plate receptors by different choline derivatives. *Proc Roy Soc Lond B* **146**: 369–381.

Erreger K, Dravid SM, Banke TG, Wyllie DJA, Traynelis SF (2005). Subunit specific gating controls rat recombinant NR1/NR2A and NR1/NR2B channel kinetics and synaptic signalling profiles. *J Physiol (London)* **563**: 345–358.

Evans RH, Francis AA, Jones AW, Smith DA, Watkins JC (1982). The effects of a series of omega-phosphonic alpha-carboxylic amino acids on electrically evoked and excitant amino acid-induced responses in isolated spinal cord preparations. *Br J Pharmacol* **75**: 65–75.

Frizelle PA, Chen PE, Wyllie DJA (2006). Equilibrium constants for (R)-[(S)-1-(4-bromo-phenyl)-ethylamino]-(2,3-dioxo-1,2,3,4-tetrahydroquinoxalin-5-yl)-methyl]-phosphonic acid (NVP-AAM077) acting at recombinant NR1/NR2A and NR1/NR2B NMDA receptors: implications for studies of synaptic transmission. *Mol Pharmacol* **70**: 1022–1032.

Furukawa H, Singh SK, Mancussco R, Gouaux E (2005). Subunit arrangement of and function in NMDA receptors. *Nature* **438**: 185–192.

Hansen KB, Clausen RP, Bjerrum EJ, Bechmann C, Greenwood JR, Christensen C *et al*. (2005). Tweaking agonist efficacy at NMDA receptors by site-directed mutagenesis. *Mol Pharmacol* **68**: 1510–1523.

Kenakin TP (1984). The classification of drugs and drug receptors in isolated tissues. *Pharmacol Rev* **36**: 165–222.

Kinarsky L, Feng B, Skifter DA, Morley RM, Sherman S, Jane DE *et al*. (2005). Identification of subunit- and antagonist-specific amino acid residues in the *N*-methyl-D-aspartate receptor glutamate-binding pocket. *J Pharmacol Exp Therapeut* **313**: 1066–1074.

Laube B, Hirai H, Sturgess M, Betz H, Kuhse J (1997). Molecular determinants of agonist discrimination by NMDA receptor subunits: analysis of the glutamate binding site on the NR2B subunit. *Neuron* **18**: 493–503.

Laube B, Schemm R, Betz H (2004). Molecular determinants of ligand discrimination in the glutamate-binding pocket of the NMDA receptor. *Neuropharmacology* **47**: 994–1007.

Lazareno S, Birdsall NJ (1993). Estimation of competitive antagonist affinity from functional inhibition curves using the Gaddum, Schild and Cheng-Prusoff equations. *Br J Pharmacol* **109**: 1110–1119.

Leff P, Dougall IG (1993). Further concerns over Cheng-Prusoff analysis. *Trends Pharmacol Sci* **14**: 110–113.

Lew MJ, Angus JA (1995). Analysis of competitive agonist–antagonist interactions by non-linear regression. *Trends Pharmacol Sci* **16**: 328–337.

Lewis TM, Sivilotti LG, Colquhoun D, Gardiner RM, Schoepfer R, Rees M (1997). Properties of human glycine receptors containing the hyperekplexia mutation α1(K276E), expressed in *Xenopus* oocytes. *J Physiol (London)* **507**: 25–40.

Mayer ML (2006). Glutamate receptors at atomic resolution. *Nature* **440**: 456–462.

Rang HP (2006). The receptor concept: pharmacology's big idea. *Br J Pharmacol* **147**: S9–S16.

Schild HO (1947). pA, a new scale for the measurement of drug antagonism. *Br J Pharmacol Chemother* **2**: 189–206.

Schild HO (1949). pA_x and competitive drug antagonism. *Br J Pharmacol Chemother* **4**: 277–280.

Wyllie DJA, Johnston AR, Lipscombe D, Chen PE (2006). Single-channel analysis of a point mutation of a conserved serine residue in the S2 ligand binding domain of the NR2A NMDA receptor. *J Physiol (London)* **574**: 477–489.

Appendix

The scheme shown in Figure 1a is the starting point for the derivation of equation (2). At equilibrium, the rates of forward and backward reactions are equal and for A binding to R we can write:

$$[A][R] = K_A[AR]$$

As it is a bit unusual to talk about a '*concentration*' of receptors in a particular state, we will use the term '*proportion*' instead. Thus, we shall denote the proportion of receptors not occupied by either agonist (A) or antagonist (B) as p_R, those occupied by agonist as p_{AR} and those by antagonist as p_{BR}. The proportion of receptors in the active state (AR*) is denoted by p_{AR*}. In addition, using the notation given in equation (1) for normalized concentration we can re-write this equation as

$$p_{AR} = p_R\ c_A \qquad (A.1)$$

Similarly, for B binding to R we have:

$$p_{BR} = p_R\ c_B \qquad (A.2)$$

and for the isomerization reaction of the agonist-occupied inactive to active state we have

$$p_{AR^*} = p_{AR}\ E \qquad (A.3)$$

In addition, the receptor must exist in one of the four states shown in the scheme and for convenience we can normalize the total receptor population to unity. Therefore, we have

$$p_R + p_{AR} + p_{BR} + p_{AR^*} = 1 \qquad (A.4)$$

We can solve for p_{AR^*} by rearranging equations (A.1–A.3) to give:

$$p_R = \frac{p_{AR}}{c_A} = \frac{p_{AR^*}}{E\ c_A},\ p_{AR} = \frac{p_{AR^*}}{E} \quad \text{and} \quad p_{BR} = \frac{p_{AR^*}\ c_B}{E\ c_A}$$

Substituting in equation (A.4) we get:

$$1 = p_{AR^*} + \frac{p_{AR^*}}{E\ c_A} + \frac{p_{AR^*}}{E} + \frac{p_{AR^*}\ c_B}{E\ c_A}$$

This can be re-written as

$$1 = \frac{p_{AR^*}\ E\ c_A + p_{AR^*} + c_A\ p_{AR^*} + p_{AR^*}\ c_B}{E\ c_A}$$

Collecting terms, we obtain

$$1 = \frac{p_{AR^*}(E\ c_A + 1 + c_A + c_B)}{E\ c_A}$$

Thus,

$$p_{AR^*} = \frac{E\ c_A}{(E\ c_A + 1 + c_A + c_B)} = \frac{E\ c_A}{1 + c_B + c_A(1 + E)}$$